Chapter 10
Extraction of Hydroxyapatite from Bovine Bone for Sustainable Development

Emon Barua, Payel Deb, Sumit Das Lala and Ashish B. Deoghare

1 Introduction

Tissue engineering is an interdisciplinary branch of science that combines the principle of engineering and basic science for biomedical applications. The primary aim of tissue engineering (TE) is to fabricate biological alternatives that help in restoring, maintaining, and improving tissue functions [1]. Tissue damage is a major health concern these days owing to accidents or other congenital diseases. A number of techniques have been developed to repair or replace these damage tissues which include the use of bone grafts like allograft and autograft [2]. Allograft is a bone or tissue that is transplanted from one person to another. The major drawback of this tissue replacement is that there is always a risk of rejection or tissue growth failure, donor shortage, and the process is highly expensive. However, autograft is a bone or tissue that is transferred from one part of the body to the other in the same person's body. But the major limitations of this tissue replacement are post-operation pains and longer time of recovery from the second surgery [3]. This has lead to the development of artificial bone material such as tissue engineered scaffold which can repair damage tissue and act as a template for tissue growth.

E. Barua · P. Deb (✉) · S. Das Lala · A. B. Deoghare
Department of Mechanical Engineering, National Institute of Technology, Silchar 788010, Assam, India
e-mail: payeldebmech13@gmail.com

E. Barua
e-mail: imon18enator@gmail.com

S. Das Lala
e-mail: sumitdaslala@gmail.com

A. B. Deoghare
e-mail: ashishdeoghare@gmail.com

P. S. Bains et al. (eds.), *Biomaterials in Orthopaedics and Bone Regeneration*, Materials Horizons: From Nature to Nanomaterials,
https://doi.org/10.1007/978-981-13-9977-0_10

A number of biomaterials have emerged, in recent years, [4] for the development of artificial bone materials. Among them, hydroxyapatite (HAp) has gained huge attention from researchers and scientists working in the field of medical science. HAp is a calcium-phosphate-based ceramic compound having excellent biocompatibility, easily tunable physical–chemical properties, non-toxicity, excellent storage stability, and inertia to microbial degradation [5]. It has similar properties to that of human bone and is finding the utmost importance in the field of orthopedics and dental implants [6]. HAp can be synthesized either synthetically from different reagents and chemicals or can be extracted from various natural resources.

Although synthetic HAp shows the exact stoichiometric ratio of calcium and phosphate similar to human bone, naturally synthesized HAp shows better cell adhesion and proliferation compared to synthetic HAp [7]. HAp extracted from natural resources such as fish scale, chicken bone, and eggshell show good biocompatibility, presence of desired minerals attached to it and non-toxicity which make it suitable for medical applications. Ho et al. [8] developed hydroxyapatite from eggshells by solid-state reactions between eggshell powders and dicalcium phosphate dihydrate ($CaHPO_4 2H_2O$, DCPD) as well as calcium pyrophosphate ($Ca_2P_2O_7$) which shows traces of different mineral components like Na, Mg, and Sr in the synthesized HAp. Panda et al. [9] extracted HAp from *Labeo rohita* and *Catla catla* fish scale and compared it with the HAp prepared from simulated body fluid (SBF) using wet precipitation method. The biocompatibility test confirms that HAp obtained from fish scales are physicochemically and biologically equivalent to the HAp chemically synthesized from SBF. Rajesh et al. [10] extracted hydroxyapatite from chicken bone bio-waste. The researchers concluded that the temperature range from 600 to 1000 °C shows the removal of organic matters from chicken bone leaving behind HAp ceramic. Therefore, chicken bone bio-waste can be a suitable bio-resource for extraction of HAp for bone tissue engineering. Rana et al. [11] extracted HAp from bovine bones by annealing the bones at high temperature. Similarly, Khoo et al. [12] derived crystalline HAp by the calcination of bovine femur at different temperatures and found that calcination temperature above 700 °C is suitable for deriving HAp for bone tissue engineering applications. However, the effect of deproteinization of bones prior to calcination was not considered in their study which has a significant effect on the properties of the synthesized HAp. Moreover, the percentage yield of HAp extracted from bovine bone was not explored by the researchers.

In the present study, an attempt is made to extract HAp from bovine bone bio-waste using thermal decomposition method. The bones are degreased and deproteinized by immersing in acetone and acid solution simultaneously one after another before heat treatment. The developed HAp is found to have improved crystallographic properties compared to the HAp synthesized by Rana et al. [11] and Khoo et al. [12], which can be a potential value-added product from bone bio-waste for biomedical applications.

2 Materials and Methods

2.1 *Thermal Decomposition of Bovine Bone for HAp Extraction*

Bovine bones were collected and washed thoroughly with tap water to remove debris, foreign materials, and impurities adhered on its surface. The washed bones were at first degreased by dipping in acetone solution in room temperature for 24 h. Since acetone is a non-polar solution, it can dissolve non-polar fat completely thereby degreasing bone materials. The bones were washed thoroughly with distilled water and were crushed into smaller pieces. Deproteinization of the crushed bones was carried out by immersing the bones in 1(N) HCl solution for 24 h. The amino acids that were building units of proteins get dissolved in HCl solution completely thereby deproteinizing the bones. The bones were then dried in room temperature for 24 h. Thereafter, they were oven dried in a hot air oven at 70 °C for 48 h. Finally, the bones were calcined at 1000 °C for 3 h using muffle furnace to obtain HAp ceramic. The detailed pictorial representation adopted for the extraction of HAp from bovine bones is depicted in Fig. 1.

2.2 *Confirmation Test for HAp Formation*

The formation of HAp was tested using XRD and FTIR analysis.

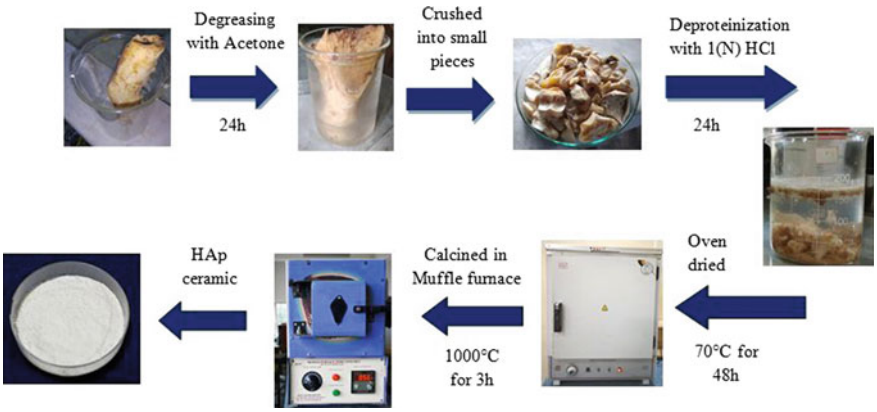

Fig. 1 Process followed for the calcination of bovine bone to extract HAp

2.2.1 X-Ray Diffraction (XRD)

It is an analytical technique adopted for the identification of phase in a crystalline material and provides crystal dimensions. The basic principle of XRD is interference occurring between the monochromatic X-rays and a crystalline material as shown in Fig. 2. The X-rays originate from cathode tube and are directed toward the finely powdered samples placed on the sample holder. The X-ray when interacts with the sample produces diffracted rays that are counted, detected, and processed.

The crystalline structure and the phase composition of the calcined powder were determined using X-ray diffractometer of PANalytical Model-X'Pert Pro. The scanning angle range was varied from 20° to 60°. The working voltage and current were set to 40 kV and 20 mA with a counting time of 2 s/step.

Phase identification was done by comparing the experimental XRD pattern to standards complied by the International Centre for Diffraction Data (ICDD) using card no. 09-0432 for hexagonal HAp structure. ICDD is a non-profit scientific organization solely devoted to collection, publishing, and distribution of diffraction pattern for the identification of materials. Patterns may be obtained through experimentation or determined based on the computation on crystal structure and Bragg's law.

The crystallite size of the HAp particles was calculated from Scherer equation as shown in Eq. 1 [13].

$$\tau = \frac{K\lambda}{\beta \cos\theta} \tag{1}$$

where,

τ Mean size (nm)
K Dimensionless shape factor 0.9
λ Wavelength (nm)
β Line broadening at half the maximum intensity (FWHM) (degree)
θ Bragg angle (degree)

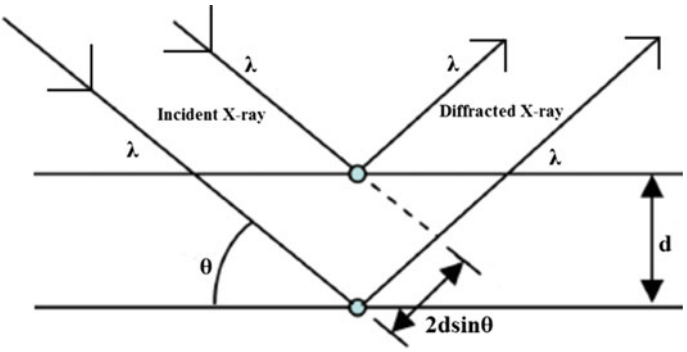

Fig. 2 Basic principle of XRD

Each atom in a crystal is represented as a single point that is joined to the other atom by line. The lattice is sub-divided into similar blocks. The interconnecting edges of unit cells define a set of crystallographic axes. The Miller indices are obtained by the intersection of the axes and plane. The reverse of the above intercepts is computed to obtain Miller indices (hkl). These hkl planes obtained from the XRD plots represent the orientation of atoms. Five high-intensity peaks corresponding to hkl planes (002), (211), (112), (300), and (222) were considered to calculate average crystallite size of HAp particle.

The percentage crystallinity was calculated from Eq. 2 as reported by Landi et al. [14] and Pang and Bao [15]. It gives the measure of degree of crystallinity of HAp particle.

$$X_c = 1 - \frac{V_{112/300}}{I_{300}} \tag{2}$$

where,

X_c Degree of crystallinity
I_{300} Intensity of 300 plane
$V_{112/300}$ Intensity of the valley between 300 and 112 planes.

2.2.2 Fourier-Transform Infrared Spectroscopy (FTIR)

It is a technique to obtain infrared spectrum of a material. The spectrum is generated by vibrational motion of the bonds present in molecules. The vibration can be either stretching or bending depending upon the nature of molecule. Stretching vibration occurs due to the change in inter-atomic distance along bond axis and bending vibration occurs due to the change in angle between two bonds in a molecule. The spectrometer accumulates these high-resolution vibrational data over wide range of spectra. Thus, it detects the presence of organic, inorganic, and biological compounds in a material.

FTIR analysis was conducted on Spectrum one FTIR spectrometer with a scan range varying from MIR 400–4000 cm^{-1} and resolution of 1.0 cm^{-1}. The analysis was conducted on FTIR system of Make-Bruker and Model-3000 Hyperion Microscope using KBr pellet technique. The reason for using KBr in FTIR analysis was its wide spectral range.

2.3 Morphological Characterizations of Synthesized HAp

SEM and TEM micrographs revealed the morphology, particle size, and nature of particle distribution of the synthesized HAp.

2.3.1 Scanning Electron Microscopy (SEM)

Scanning electron microscopy provides images of surface by using focused beam of electron. SEM is used to evaluate grain size, particle size, and material homogeneity. Scanning electron microscope of make Quanta 200F and model FEI was used to examine the morphology of synthesized HAp. The instrument has a magnification range of minimum 12× to maximum 100,000×. Sample was coated by a thin conductive layer of gold using gold sputter machine. A sputtering machine of make Cressington-108 auto and Model No.: 7006-8 was used for gold coating of samples using a vacuum pump. The samples were analyzed at 20 kV with a magnification range of 500–30,000×.

2.3.2 Transmission Electron Microscopy (TEM)

TEM analysis accounts for a beam of electron to be directed on a specimen. The thickness of the specimen is basically less than 100 nm or in the form of grid. The interaction of the beam of electrons on the surface of the specimens generates images. TEM has comparatively higher resolution compared to other microscopy that enables it to capture finer details even at atomic levels.

The morphology and the microstructure of the HAp derived from Bovine bones were investigated using transmission electron microscope of Make JEM-100 CX II. The machine operates at 100 kV. The particle size was calculated from TEM images using ImageJ software. It is an open-source software used for multidimensional images. It can measure distances and angles, display, edit, analyze, and process images.

2.4 Thermal Characterization of the Synthesized HAp

The high thermal stability of the HAp derived from Bovine bone was confirmed from TG analysis.

2.4.1 Thermo Gravimetric Analysis (TGA)

The thermal stability of the HAp was examined through TG analysis. Basic principle of TGA is to measure the mass of substance as a function of time. The analysis is carried out to evaluate changes in mass, thermal stability, oxidation/reduction behavior, and decomposition [16]. TGA was conducted on NETZSCH STA 449 F3 Jupiter in the mixed environment of nitrogen and oxygen to investigate the weight loss due to heating. To ascertain the test, 20 mg HAp was heated from 30 to 900 °C to investigate the weight loss on heating. The rate of heating was maintained at 10 °C/min.

3 Results and Discussion

3.1 X-Ray Diffraction Analysis

XRD spectrum of the synthesized powder is shown in Fig. 3. The diffraction patterns reveal HAp was the only phase found in the calcined powder. The peaks were sharp which indicates the highly crystalline nature of HAp. The extracted HAp from bovine bones showed an average crystallite size of 30.39 nm which is smaller than the ones obtained by Khoo et al. [12]. Further, the synthesized HAp showed 80.4% crystallinity which corresponds to a high degree of crystal formation [11]. Since smaller crystallite size with high degree of crystallinity is much desirable in HAp for tissue engineering applications [17], therefore it can be concluded that acid pre-treatment of bovine bone results in better deproteinization which enhances the crystallographic properties of the extracted HAp. Similar observation was reported by Deb et al. [18], which reveals that acid pre-treatment of fish scales yields HAp with better properties.

3.2 Fourier-Transform Infrared Spectroscopy Analysis

FTIR spectrum of the synthesized powder is shown in Fig. 4. The spectra showed peaks at 1530 and 1650 cm^{-1} which confirmed the presence of carbonate ions (CO_3^{2-}) [19]. The absorbance peak at 570 and 1021 cm^{-1} corresponds to the υ4 and υ3 P–O stretching vibration of PO_4 group, respectively [20]. Similarly, the band at 3570 cm^{-1} attributed to the characteristic stretching modes of hydroxyl groups (O–H) [21]. The presence of the absorbance peaks corresponding to phosphate,

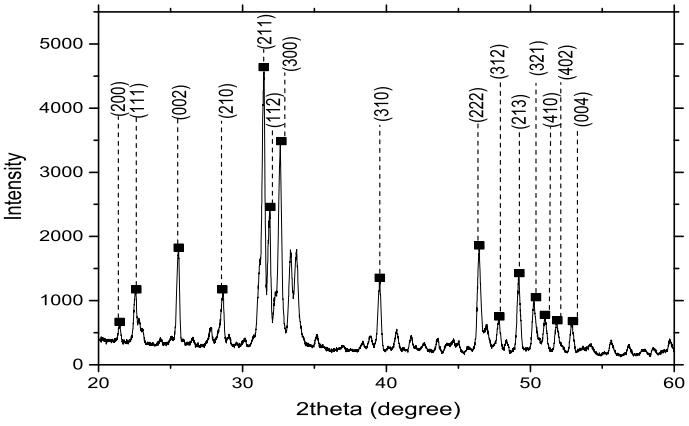

Fig. 3 XRD spectrum of bovine bone HAp

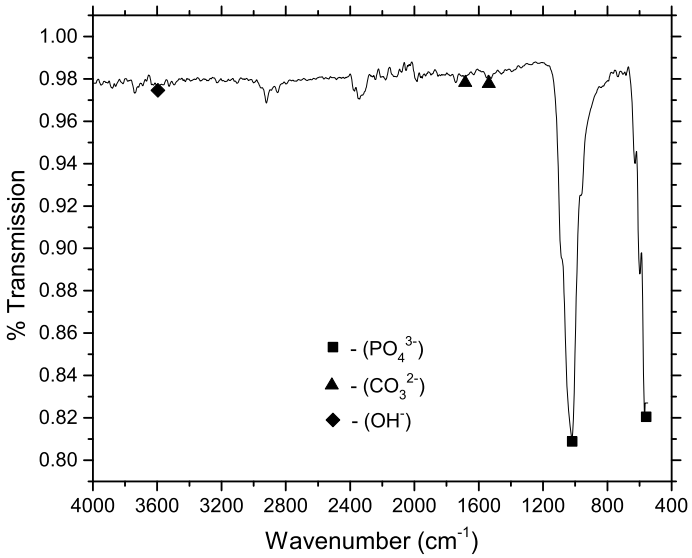

Fig. 4 FTIR spectra of synthesized HAp

carbonate, and hydroxyl group confirmed the formation of hydroxyapatite in the calcined powder.

3.3 Scanning Electron Microscopy Analysis

SEM micrograph of synthesized HAp ceramic is represented in Fig. 5a. Formation of needle-like HAp flakes was observed from the SEM image on calcination at 1000 °C. Similar observation of HAp flake formation was also reported by Barakat

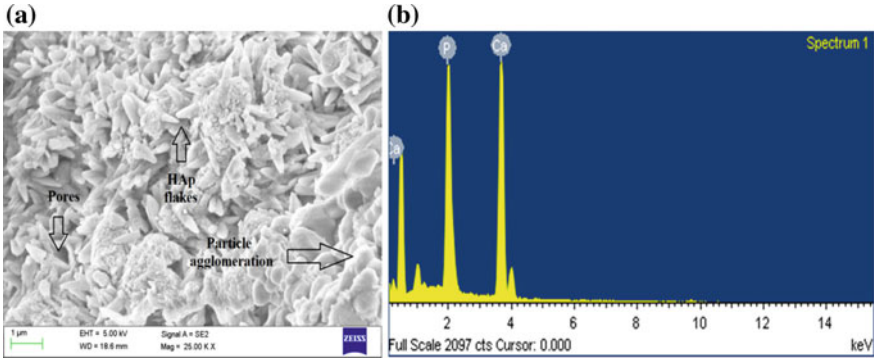

Fig. 5 **a** SEM micrograph and **b** EDX spectra of synthesized HAp

et al. [22]. Particle agglomeration with porous morphology was also observed for the synthesized HAp which is due to the high calcination temperature during HAp synthesis [23]. The formation of porous morphology and agglomerated HAp particle is best suited for biomedical applications. EDX spectra of the HAp shown in Fig. 5b further confirmed the existence of Ca and P in the calcined powder. The ratio of Ca/P observed from EDX analysis was found to be 1.71 which is fairly accurate with the stoichiometric ratio (1.67) of the pure HAp.

3.4 Transmission Electron Microscopy Analysis

TEM micrograph of the bovine-bone-derived HAp is depicted in Fig. 6 which showed rod-shaped HAp particles. The particle size of the synthesized HAp measured using ImageJ software was found to be approximately 68 nm. Selected area electron diffraction (SAED) pattern for the extracted HAp showed bright spots with concentric rings which indicate the presence of ultra-fine crystalline powder particles. This implied polycrystalline nature of HAp [24].

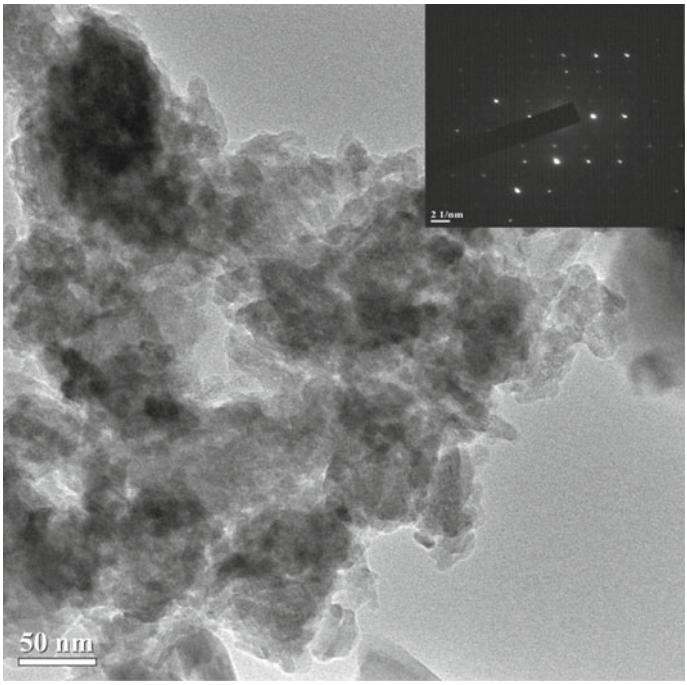

Fig. 6 TEM image of synthesized HAp

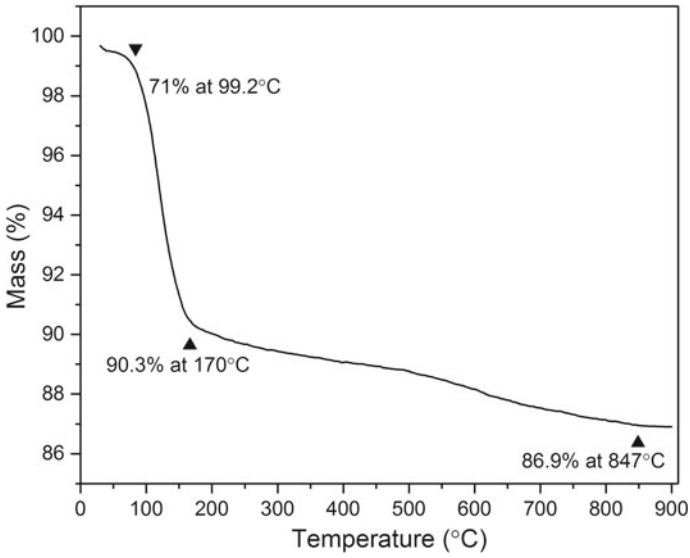

Fig. 7 TGA curve for the synthesized HAp

3.5 TGA Results

TGA curve corresponding to weight loss of the HAp with respect to temperature is represented in Fig. 7. A minor degradation was observed up to 170 °C which is due to the presence of entrapped moisture. Minor degradation was further observed up to 847 °C that might correspond to the presence of any traces of organic matter. However, above 847 °C, there was almost no degradation of HAp which confirmed high thermal stability of the synthesized HAp [25]. It was also observed that there was only 13.1% degradation of HAp keeping residual mass of 86.9% that further confirmed high thermal stability of the synthesized HAp.

3.6 Quantification of Extracted HAp

The yield of the extracted HAp was calculated by measuring the dry weight of the raw bone considered before the process and the HAp extracted from it. Details of the weight measured during the formation of HAp from bovine bone are depicted in Table 1.

Table 1 Percentage yield of the HAp synthesized from bovine bone

Weight of raw dry bone (g)	Weight after cleaning with acetone (g)	Weight after deproteinization (g)	Weight after calcination (HAp obtained) (g)	% yield
35	29.683	19.587	8.159	23.31

4 Conclusions

In the present study an attempt is made to synthesize nano-sized hydroxyapatite from bovine bone bio-waste by acid pre-treatment of bones followed by calcination at 1000 °C. The calcined powder obtained was characterized by FTIR and XRD analysis that confirms the successful formation of HAp. Intense and sharp peaks of XRD pattern imply crystalline nature of the synthesized HAp. Smaller crystallite size of 30.39 nm with 80.4% crystallinity shows enhanced crystallographic properties of the extracted HAp for biomedical applications. Presence of carbonate, phosphate, and hydroxyl ions corresponds to the formation of HAp in the calcined powder. Agglomerated HAp flakes with porous morphology are observed from SEM micrograph. TEM image reveals the formation of rod-shaped HAp particle with average size of 68 nm. SAED pattern indicates concentric rings with shiny spots confirming polycrystalline nature of HAp. High thermal stability with no degradation above 700 °C is shown in TGA curve for the synthesized HAp. Thus, acid pre-treated bovine bones yield HAp with enhanced properties that can have wide applications in the development of artificial bone material, bone void fillers for orthopedic, coating of orthopedic implants, drug delivery and in various other biomedical applications.

Acknowledgements The authors acknowledge Material Science Laboratory of Mechanical Engineering Department, NIT Silchar, for performing TG analysis. The authors thank SAIF, IIT Madras, Chennai, for performing SEM and FTIR analysis. The authors are grateful to SAIF, Gauhati University and CIF, NIT Silchar for XRD analysis of samples. The authors thank Indovation Laboratory and TEQIP III, NIT Silchar, for providing fund for the characterizations of the samples.
Ethical approval No Human/animal testing was performed during this study.

References

1. Deb P, Deoghare AB, Borah A, Barua E, Lala SD (2018) Scaffold development using biomaterials: a review. Mater Today: Proc 5(5):12909–12919
2. Barua E, Deoghare AB, Deb P, Lala SD (2018) Naturally derived biomaterials for development of composite bone scaffold: a review. IOP Conf Ser: Mater Sci Eng 377(1):012013
3. Wang W, Yeung KWK (2017) Bioactive materials bone grafts and biomaterials substitutes for bone defect repair: a review. Bioact Mater 2(4):224–247
4. Bhui AS, Singh G, Sidhu SS, Bains PS (2018) Experimental investigation of optimal ED machining parameters for Ti-6Al-4 V biomaterial. FU Mech Eng 16(3):337–345
5. Lin K, Chang J (2015) Structure and properties of hydroxyapatite for biomedical applications. HAp Biomed Appl 4214(8):3–19

6. Muhammad N, Gao Y, Iqbal F, Ahmad P, Ge R, Nishan U, Rahim A, Gonfa G, Ullah Z (2016) Extraction of biocompatible hydroxyapatite from fish scales using novel approach of ionic liquid pretreatment. Sep Purif Technol 161(7):129–135
7. Mondal S, Mondal A, Mandal N, Mukhopadhyay SS, Dey A, Singh S (2014) Physico-chemical characterization and biological response of Labeo rohita-derived hydroxyapatite scaffold. Bioprocess Biosyst Eng 37(7):1233–1240
8. Ho WF, Hsu HC, Hsu SK, Hung CW (2013) Calcium phosphate bioceramics synthesized from eggshell powders through a solid state reaction. Ceram Int 39(6):6467–6473
9. Panda NN, Pramanik K, Sukla LB (2014) Extraction and characterization of biocompatible hydroxyapatite from fresh water fish scales for tissue engineering scaffold. Bioprocess Biosyst Eng 37(3):433–440
10. Rajesh R, Hariharasubramanian A, Ravichandran YD (2012) Chicken bone as a bioresource for the bioceramic (Hydroxyapatite). Phosphorous, Sulfur Silicon Relat Elem 187(8):914–925
11. Rana M, Akhtar N, Rahman S, Jamil HM, Asaduzzaman SM (2017) Extraction of hydroxyapatite from bovine and human cortical bone by thermal decomposition and effect of gamma radiation: a comparative study. Int J Comple Altern Med 8(3):00263
12. Khoo W, Nor FM, Ardhyananta H, Kurniawan D (2015) Preparation of natural hydroxyapatite from bovine femur bones using calcination at various temperatures. Proc Manuf 2:196–201
13. Gautam CR, Tamuk M, Manpoong CW, Gautam SS, Kumar S, Singh AK, Mishra VK (2016) Microwave synthesis of hydroxyapatite bioceramic and tribological studies of its composites with $SrCO_3$ and ZrO_2. J Mater Sci 51(10):4973–4983
14. Landi E, Tampieri A, Celotti G, Sprio (2000) Densification behaviour and mechanisms of synthetic hydroxyapatites. J Euro Ceram Soc 20:2377–2387
15. Pang YX, Bao X (2003) Influence of temperature, ripening time and calcination on the morphology and crystallinity of hydroxyapatite nanoparticles. J Euro Ceram Soc 23(10):1697–1704
16. Bains PS, Payal HS, Sidhu SS (2017) Analysis of coefficient of thermal expansion and thermal conductivity of bi-modal SiC/A356 composites fabricated via powder metallurgy route. https://doi.org/10.1115/ht2017-5122
17. Boudemagh D, Venturini P, Fleutot S, Cleymand F (2018) Elaboration of hydroxyapatite nanoparticles and chitosan/hydroxyapatite composites : a present status. Polym Bull. https://doi.org/10.1007/s00289-018-2483-y
18. Deb P, Deoghare AB (2019) Effect of pretreatment processes on physicochemical properties of hydroxyapatite synthesized from *Puntius conchonius* fish scales. Bull Mater Sci 42(3):1–9
19. Zhang Y, Yokogawa Y (2008) Effect of drying conditions during synthesis on the properties of hydroxyapatite powders. J Mater Sci Mater Med 19(2):623–628
20. Destainville A, Champion E, Laborde E (2003) Synthesis, characterization and thermal behavior of apatitic tricalcium phosphate. Mater Chem Phys 80(1):269–277
21. Wei M, Evans JH, Bostrom T, Grondahl L (2003) Synthesis and characterization of hydroxyapatite, fuoride-substituted hydroxyapatite and fuorapatite. J Mater Sci Mater Med 14(4):311–320
22. Sheikh FA, Yong H (2009) Extraction of pure natural hydroxyapatite from the bovine bones bio waste by three different methods. J Mater Process Technol 209:3408–3415
23. Manalu JL, Soegijono B, Indrani DJ (2015) Characterization of hydroxyapatite derived from bovine bone characterization of hydroxyapatite derived from bovine. Asian J Appl Sci 3(4):758–765
24. Xu JL, Khor KA, Dong ZL, Gu YW, Cheang P (2004) Preparation and characterization of nano-sized hydroxyapatite powders produced in a radio frequency (rf) thermal plasma. Mater Sci Eng, A 374(1–2):101–108
25. Mondal S, Mahata S, Kundu S, Mondal B (2010) Processing of natural resourced hydroxyapatite ceramics from fish scale. Adv Appl Ceram 109(4):234–239